Copyright © 2011 Tech Science Press CMC, vol.21, no.2, pp.119-146, 2011

Stress Distribution in an Infinite Body Containing Two Neighboring Locally Curved Nanofibers

Surkay D. Akbarov[1,2], Resat Kosker[3] and Nihan T. Cinar[3]

Abstract: In the present paper, the stress distribution in an infinite elastic body containing two neighboring nanofibers is studied. It is assumed that the midlines of the fibers are in the same plane. With respect to the location of the fibers according to each other the co-phase and anti-phase curving cases are considered. At infinity uniformly distributed normal forces act in the direction of the nanofibers' location. The investigations are carried out in the framework of the piecewise homogeneous body model with the use of the three-dimensional geometrically non-linear exact equations of the theory of elasticity. The normal and shear self-equilibrated stresses arising as a result of the nanofiber curving are analyzed. In particular, the influence of the interaction between the fibers on the distribution of these stresses is studied. A lot of numerical results on the effect of the geometrical non-linearity to the values of the self balanced shear and normal stresses are presented.

Keywords: Nanocomposite, nanofibers, Self balanced stresses, geometrical non-linearity, local curving.

1 Introduction

One of the basic factors determining the strength of unidirectional fibrous composites along the fiber direction is the curvature of the fibers. The curvature may occur as a result of design (see: Akbarov and Guz (2000), Chou, Cullough and Pipes (1986), Feng, Allen and Moy (1998), Ganesh and Naik (1996), Tarnopolsky, Jigun and Polyakov (1987)) or as a consequence of some technological process (see:

[1] Corresponding author. Yildiz Technical University, Faculty of Mechanical Engineering, Department of Mechanical Engineering, Yildiz Campus, 34349, Besiktas, Istanbul-Turkey, akbarov@yildiz.edu.tr.

[2] Institute of Mathematics and Mechanics of National Academy of Sciences of Azerbaijan, 37041, Baku, Azerbaijan.

[3] Yildiz Technical University, Faculty of Chemistry and Metallurgy, Department of Mathematical Engineering, Davutpasa Campus No:127 Topkapi 34010, Istanbul, TURKEY.

Corten (1967), Tomashevskii and Yakovlev (2004)). The curvature caused by design features is modeled as a periodical, whereas the curvature caused by the technological process is modeled as a local one. An efficient practical employment of unidirectional fibrous composite materials under service conditions requires intensive systematic investigations to determine the stress-strain state in these materials, with account of curving in reinforcing fibers. For this purpose, within the framework of a piecewise homogenous body model by the use of the three dimensional exact equations of the theory of the elasticity, a method is developed to investigate the stress-strain state in the unidirectional composites (Akbarov and Guz (1985a, 1985b)). This method is employed in the case where the curving of the fibers is periodic. The reviews of the results obtained by this method are detailed in the papers by Akbarov and Guz (2002, 2004).

The method considered in Akbarov and Guz (1985a) is presented for the case where the concentration of the fibers is too small and the interactions between them are neglected. In Kosker and Akbarov (2003), this method is developed for two neighboring periodically curved fibers and some numerical results are given. In Akbarov and Kosker (2003a, 2003b), the mentioned method is extended to the geometrical nonlinear statement and numerical results obtained for one and two neighboring periodically curved fibers are presented. The problem regarding to the corresponding stability problems is studied in Akbarov and Kosker (2004) and the review of the investigations mentioned stability problems is giving in Akbarov (2007). In Akbarov, Kosker and Ucan (2004, 2006) the foregoing approach was developed for a periodically located row of fibers in an infinite matrix and corresponding numerical results were presented. In the paper Akbarov, Kosker and Ucan (2004) (Akbarov, Kosker and Ucan (2006)) it was assumed that the curving of the fibers relative to each other is sinphase (antiphase) one and the investigations were made within the framework of the linear theory of elasticity. In connection with this in Akbarov, Kosker and Ucan (2010) the investigation carried out in Akbarov, Kosker and Ucan (2004, 2006) is developed for the geometrical non-linear statement.

Local curving of the fibers is considered also in Djafarova (1992, 1994, 1995) in the case of low fiber concentration and when their interaction is neglected. Moreover, the linear theory of elasticity was used in these investigations. According to well-known mechanical considerations and the results obtained in Akbarov and Kosker (2003a, 2003b), it is seen that the geometrical nonlinearity affects the self-balanced stresses caused by fiber carvings'. Therefore in Akbarov, Kosker and Simsek (2005), geometrical nonlinear statement is adopted as in Djafarova (1992, 1994, 1995). It is assumed that the fiber concentration is smaller and any interaction between the fibers is disregarded. Therefore, the composite is modeled as an infinite body containing a single locally curved fiber and some numerical results on

the distribution of the self-balanced stress which are as a result of the local curving of the fiber are presented.

The changeover from the microlevel to the nanolevel in the science of materials broke new ground in the mechanics of materials and structures. This was preceded by important events in the physics and chemistry of nanoformations, which were partially described in Guz (2006), Guz, Rushchitsky and Guz (2007), a basic approach to study the mechanical properties of nanocomposite materials with polymer matrix was proposed and the deformation of nanocomposites and structural members made of them. Nanofibers are differed from the microfibers by the value of ratio $\mathrm{E}^{(f)}/\mathrm{E}^{(m)}$ where $\mathrm{E}^{(f)}$ ($\mathrm{E}^{(m)}$) is a modulus of elasticity of the fibers (matrix) material. If its value is $300 \leq E^{(f)}/E^{(m)} \leq 1000$, then fibers are defined as the polymer matrix+nanofiber (see: Qian, Dickey, Andrews and Rantell (2000), Zhuk and Guz (2007), Guz and Dekret (2008), Maligino, Warrior and Long (2009)).

However, in papers Kosker and Cinar (2009) and Cinar, Kosker, Akbarov and Akat (2010) the stress distributions in an infinite elastic body containing two neighboring cophase locally curved fibers (which are located along two parallel lines in the same plane (Kosker and Cinar (2009)) and in the out of plane (Cinar, Kosker, Akbarov and Akat (2010))) and between which the interaction is taking into account. It was considered the case where the fibers are micro-fibers. In the present paper the investigations carried out in Kosker and Cinar (2009) and Cinar, Kosker, Akbarov and Akat (2010) is extended for the case where the fibers are nanofibers and assumed that the middle lines of the fibers lie on the same plane. It is considered not only cophase curving case (as in Kosker and Cinar (2009), Cinar, Kosker, Akbarov and Akat (2010)), but also antiphase curving case. The investigations are carried out in the framework of the piecewise homogeneous body model, with the use of the three dimensional geometrically nonlinear exact equations of the theory of elasticity for determination of the stress distribution (the normal and shear stresses acting along the nanofibers) in the nanocomposites with unidirectional locally curved two neighboring nanofibers. The numerical results related to stress distribution in considered body and influence of geometrical nonlinearty to this distribution are presented and interpreted.

Throughout the investigations, repeated indices are summed over their ranges; however, underlined repeated indices are not summed. Furthermore, to simplify the consideration we will use the tensor notation and physical components of tensors simultaneously.

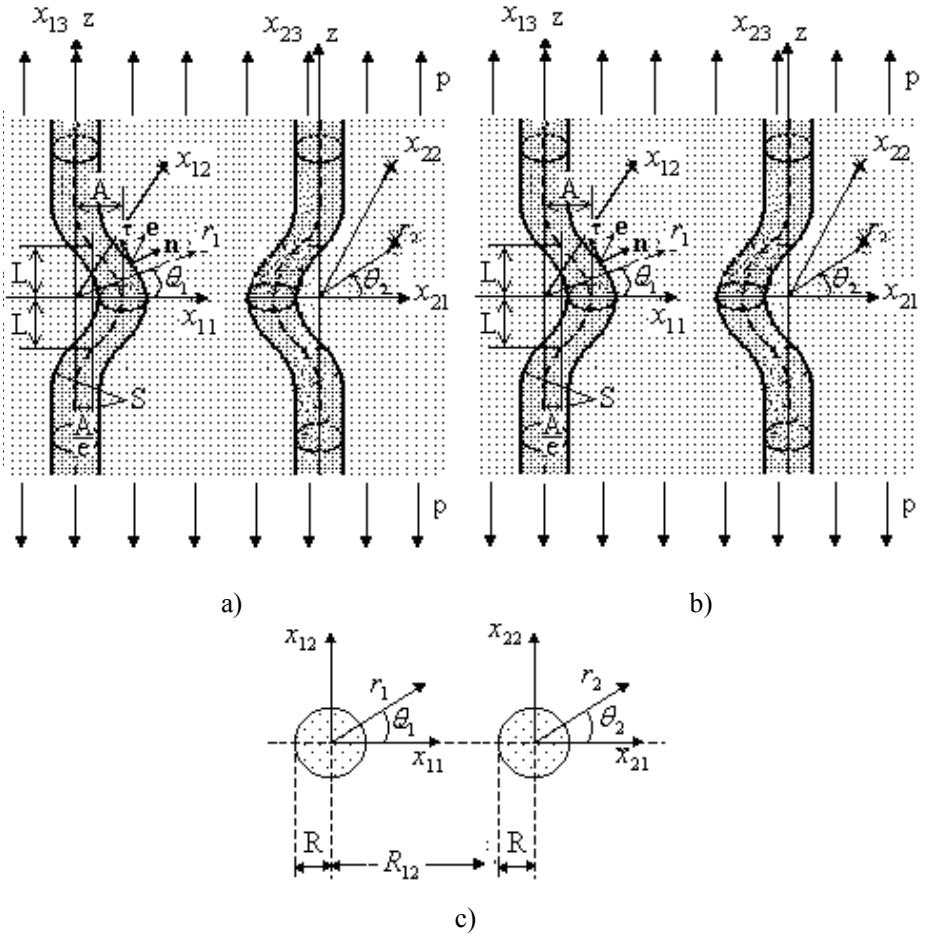

Figure 1: The geometry of material structure a) co-phase curving; b) antiphase curving and c) chosen coordinates

2 Formulation of the problem

We consider an infinite body containing two nanofibers with an initial local imperfection. With respect to the location of the nanofibers according to each other the following two cases are considered: (I) cophase curving and (II) antiphase curving in plane. Here under "in plane" it is understood that the

midlines of the fibers lie in the same plane. With the middle line of each fiber we associate Lagrangian rectilinear $O_k x_{1k} x_{2k} x_{3k}$ and cylindrical $O_k r_k \theta_k z_k$ system

of coordinates (Fig. 1). Here k=1, 2 is related to the first and second nanofiber in turn in order. The body is compressed or stretched as $|x_{k3}| \to \infty$ by uniformly distributed normal forces with intensity p acting along the Ox_{k3} axis and the cross section of the each nanofiber normal to its axial line is a circle of constant radius R along the entire length. Below the values related to the nanofibers will be denoted by upper indices (21), (22); but those related to the matrix by upper index (1). For the nanofibers and matrix, in the geometrical nonlinear statement, we have the following governing field equations:

$$\nabla_i \left[\sigma^{(\underline{m})in} \left(g_n^j + \nabla_n u^{(\underline{m})j} \right) \right] = 0,$$

$$2\varepsilon_{jn}^{(m)} = \nabla_j u_n^{(m)} + \nabla_n u_j^{(m)} + \nabla_j u^{(\underline{m})i} \nabla_n u_i^{(\underline{m})}, \tag{1}$$

$$\sigma_{(ij)}^{(m)} = \lambda^{(\underline{m})} (e^{(\underline{m})} \delta_i^j) + 2\mu^{(\underline{m})} \varepsilon_{(ij)}^{(\underline{m})}, \;\; e^{(m)} = \varepsilon_{rr}^{(m)} + \varepsilon_{\theta\theta}^{(m)} + \varepsilon_{zz}^{(m)}$$

Also, perfect contact conditions are assumed at the fibers-matrix interfaces S_k:

$$\begin{aligned} &\sigma^{(2\underline{q})in} \left(g_n^j + \nabla_n u^{(2\underline{q})j} \right) \Big|_{S_{\underline{q}}} n_{\underline{q}(j)} = \sigma^{(1)in} \left(g_n^j + \nabla_n u^{(1)j} \right) \Big|_{S_{\underline{q}}} n_{\underline{q}(j)}, \\ &u_j^{(2\underline{q})} \Big|_{S_{\underline{q}}} = u_j^{(1)} \Big|_{S_{\underline{q}}} \end{aligned} \tag{2}$$

In equations (1) and (2), the conventional tensor notation is used and the subscripts in parentheses denote the physical components of the corresponding tensors. It is known that

$$\sigma_{(ij)} = \sigma^{\underline{ij}} H_{\underline{i}} H_{\underline{j}} = \sigma_{\underline{ij}} \frac{1}{H_{\underline{i}} H_{\underline{j}}}, \varepsilon_{(ij)} = \varepsilon^{\underline{ij}} H_{\underline{i}} H_{\underline{j}} = \varepsilon_{\underline{ij}} \frac{1}{H_{\underline{i}} H_{\underline{j}}},$$

$$u_{(i)} = u^{\underline{i}} H_{\underline{i}} = u_{\underline{i}} \frac{1}{H_{\underline{i}}}, \tag{3}$$

where $(ij) = rr, \theta\theta, zz, r\theta, rz, z\theta$, $(i) = r, \theta, z$. H_i are the Lamé coefficients, and $n_{(k)j}$ are the covariant components of the unit normal vector to the surfaces S_k (Fig.1). We define the initial imperfection form of the fiber by an equation of its axial line (Fig.1).

$$x_{k1} = F_k(x_{k3}) = \varepsilon \delta_k(x_{k3}), x_{k2} = 0,$$

$$|\delta_k(x_{k3})|, \left| \frac{d\delta_k(x_{k3})}{dx_{k3}} \right| \to 0 \text{ for } |x_{k3}| \to \infty \tag{4}$$

where ε is a small parameter $(0 \le \varepsilon < 1)$ whose geometric meaning will be indicated upon specification of this function.

3 Method of Solution

The equations of the interfaces S_k can be represented as $\vec{g}_k(r_k,\theta_k,x_{k3}) = r_k(\theta_k,t_3)\vec{e}_r + x_{k3}(\theta_k,t_3)\vec{e}_3$, in the cylindrical system of coordinates $O_k r_k \theta_k z_k$, where $\vec{e}_r$ and $\vec{e}_3$ are the unite ort vectors, t_3 is a parameter and $t_3 \in (-\infty,+\infty)$. According to the equation (4) and to the condition on the fiber cross section, the functions $r_k(\theta_k,t_3)$ and $x_{k3}(\theta_k,t_3)$ must satisfy simultaneously the following equations

$$\varepsilon\delta_{\underline{k}}(t_3)\left(r_{\underline{k}}\cos\theta_{\underline{k}} - \varepsilon\delta_{\underline{k}}(t_3)\right) + x_{k3} - t_3 = 0,$$

$$r_{\underline{k}}^2\sin^2\theta_{\underline{k}} + \left(1+\varepsilon^2(\delta'_{\underline{k}})^2\right)\left(r_{\underline{k}}\cos\theta_{\underline{k}} - \varepsilon\delta_{\underline{k}}(t_3)\right)^2 = R^2, \delta'_k(t_3) = \frac{d\delta_k(t_3)}{dt_3}$$

The first of them is the equation of the plan, the normal vector of which coincides with the tangent vector of middle line of the fiber. But the second equation represents the condition of the fiber cross-section described under problem formulation. Consequently from these equations we obtain the following expressing for the functions $r_k(\theta_k,t_3)$ and $x_{k3}(\theta_k,t_3)$

$$r_k(\theta_k,t_3) = \frac{\varepsilon\delta_k(t_3)\left(1+\varepsilon^2(\delta'_k(t_3))^2\right)\cos\theta_k}{1+(\delta'_k(t_3))^2\varepsilon^2\cos^2\theta_k} +$$

$$\left\{\frac{\varepsilon^2(\delta_k(t_3))^2\left(1+\varepsilon^2(\delta'_k(t_3))^2\right)^2\cos^2\theta_k}{\left(1+(\delta'_k(t_3))^2\varepsilon^2\cos^2\theta_k\right)^2} + R^2 - (\delta_k(t_3))^2\varepsilon^2\left(1+\varepsilon^2(\delta'_k(t_3))^2\right)\right\}^{1/2},$$

$$x_{k3}(\theta_k,t_3) = t_3 - \varepsilon\delta'_k(t_3)\left(r_k(\theta_k,t_3) - \varepsilon\delta_k(t_3)\right) \tag{5}$$

Using the well-known operations of the differential geometry, we also obtain the expression for the components n_{kr}, $n_{k\theta}$ and n_{k3} of the unit normal vector to the surface S_k from equations $\vec{g}_k(r_k,\theta_k,x_{k3}) = r_k(\theta_k,t_3)\vec{e}_r + x_{k3}(\theta_k,t_3)\vec{e}_3$ and (5). As these expressions are cumbersome, therefore they are not given here.

Taking into account that the degree of the local curving (i.e. the values of $\left|\varepsilon\delta'_k(t_3)\right| << 1$) is small, we seek quantities characterizing the stress-strain state of the matrix and the fibers in the form of series in positive powers of the small parameter ε:

$$\sigma_{rr}^{(k)} = \sum_{q=0}^{\infty}\varepsilon^q\sigma_{rr}^{(k),q},\ldots,\varepsilon_{rr}^{(k)} = \sum_{q=0}^{\infty}\varepsilon^q\varepsilon_{rr}^{(k),q},\ldots,u_r^{(k)} = \sum_{q=0}^{\infty}\varepsilon^q u_r^{(k),q},.. \tag{6}$$

The quantities r_k, z_k, n_{kr}, $n_{k\theta}$ and n_{kz} are also presented in series form:

$$r_k = R + \sum_{q=1}^{\infty}\varepsilon^q a_{rq}(R,\theta_k,t_3), z_k = t_3 + \sum_{q=1}^{\infty}\varepsilon^q a_{zq}(R,\theta_k,t_3),$$

$$n_{kr} = 1 + \sum_{q=1}^{\infty} \varepsilon^q b_{rq}(R, \theta_k, t_3), n_{k\theta} = \sum_{q=1}^{\infty} \varepsilon^q b_{\theta q}(R, \theta_k, t_3),$$

$$n_{kz} = \sum_{q=1}^{\infty} \varepsilon^q b_{zq}(R, \theta_k, t_3) \tag{7}$$

The expressions for the coefficients of the ε^q in (7) can be determined by employing some routine operations and the details are omitted.

Substituting the expression (6) in equation (1) and grouping terms with identical powers, we obtain a complete equation system for each approximation. In this case, equation (1) holds for the zeroth approximation and the equations derived for the first and subsequent approximations contain the values of the previous approximations. We assume that the materials of the matrix and fibers are comparatively rigid, and therefore the nonlinear terms can be neglected in the equations obtained for the zeroth approximation and the term $(g_n^j + \nabla_n u^{(k)j,0})$ can be replaced by δ_n^j in the first and subsequent approximations.

With these assumptions, the following equations are obtained for the first approximation.

$$\frac{\partial \sigma_{rr}^{(k),1}}{\partial r} + \frac{1}{r}\frac{\partial \sigma_{r\theta}^{(k),1}}{\partial \theta} + \frac{\partial \sigma_{rz}^{(k),1}}{\partial z} + \frac{1}{r}\left(\sigma_{rr}^{(k),1} - \sigma_{\theta\theta}^{(k),1}\right) + \frac{1}{r}\frac{\partial}{\partial r}\left(r\sigma_{rr}^{(\underline{k}),0}\frac{\partial u_r^{(\underline{k}),1}}{\partial r}\right) +$$

$$\frac{1}{r}\frac{\partial}{\partial \theta}\left[\sigma_{\theta\theta}^{(\underline{k}),0}\left(\frac{1}{r}\frac{\partial u_r^{(\underline{k}),1}}{\partial \theta} - \frac{1}{r}u_\theta^{(\underline{k}),1}\right)\right] + \frac{\partial}{\partial z}\left(\sigma_{zz}^{(\underline{k}),0}\frac{\partial u_r^{(\underline{k}),1}}{\partial z}\right) - \frac{1}{r}\left(\sigma_{\theta\theta}^{(\underline{k}),0}\left(\frac{1}{r}\frac{\partial u_\theta^{(\underline{k}),1}}{\partial \theta} + \frac{u_r^{(\underline{k}),1}}{r}\right)\right) = 0 \quad ,$$

$$\frac{\partial \sigma_{r\theta}^{(k),1}}{\partial r} + \frac{1}{r}\frac{\partial \sigma_{\theta\theta}^{(k),1}}{\partial \theta} + \frac{\partial \sigma_{\theta z}^{(k),1}}{\partial z} + \frac{2}{r}\sigma_{r\theta}^{(k),1} + \frac{1}{r}\frac{\partial}{\partial r}\left(r\sigma_{rr}^{(\underline{k}),0}\frac{\partial}{\partial r}u_\theta^{(\underline{k}),1}\right) +$$

$$\frac{1}{r}\frac{\partial}{\partial \theta}\left[\sigma_{\theta\theta}^{(\underline{k}),0}\left(\frac{1}{r}\frac{\partial u_\theta^{(\underline{k}),1}}{\partial \theta} + \frac{1}{r}u_r^{(\underline{k}),1}\right)\right] + \frac{\partial}{\partial z}\left(\sigma_{zz}^{(\underline{k}),0}\frac{\partial u_\theta^{(\underline{k}),1}}{\partial z}\right) + \frac{1}{r}\left(\sigma_{\theta\theta}^{(\underline{k}),0}\left(\frac{1}{r}\frac{\partial u_r^{(\underline{k}),1}}{\partial \theta} - \frac{1}{r}u_\theta^{(\underline{k}),1}\right)\right) = 0$$

$$\frac{\partial \sigma_{rz}^{(k),1}}{\partial r} + \frac{1}{r}\frac{\partial \sigma_{\theta z}^{(k),1}}{\partial \theta} + \frac{\partial \sigma_{zz}^{(k),1}}{\partial z} + \frac{1}{r}\sigma_{rz}^{(k),1} + \frac{1}{r}\frac{\partial}{\partial r}\left(r\sigma_{rr}^{(\underline{k}),0}\frac{\partial u_z^{(\underline{k}),1}}{\partial r}\right) +$$

$$\frac{1}{r}\frac{\partial}{\partial \theta}\left(\sigma_{\theta\theta}^{(\underline{k}),0}\frac{1}{r}\frac{\partial u_z^{(\underline{k}),1}}{\partial \theta}\right) + \frac{\partial}{\partial z}\left(\sigma_{zz}^{(\underline{k}),0}\frac{\partial u_z^{(\underline{k}),1}}{\partial z}\right) = 0 \tag{8}$$

$$\sigma_{(in)}^{(k),1} = \lambda^{(\underline{k})} e^{(\underline{k}),1}\delta_i^n + 2\mu^{(\underline{k})}\varepsilon_{(in)}^{(\underline{k}),1}, \tag{9}$$

$$e^{(k),1}=\varepsilon_{(11)}^{(k),1}+\varepsilon_{(22)}^{(k),1}+\varepsilon_{(33)}^{(k),1},\varepsilon_{rr}^{(k),1}=\frac{\partial u_r^{(k),1}}{\partial r},\varepsilon_{\theta\theta}^{(k),1}=\frac{\partial u_\theta^{(k),1}}{r\partial\theta}+\frac{u_r^{(k),1}}{r},$$

$$\varepsilon_{zz}^{(k),1}=\frac{\partial u_z^{(k),1}}{\partial z},\varepsilon_{r\theta}^{(k),1}=\frac{1}{2}\left(\frac{\partial u_r^{(k),1}}{r\partial\theta}+\frac{\partial u_\theta^{(k),1}}{\partial r}-\frac{u_\theta^{(k),1}}{r}\right),$$

$$\varepsilon_{\theta z}^{(k),1}=\frac{1}{2}\left(\frac{\partial u_\theta^{(k),1}}{\partial z}+\frac{\partial u_z^{(k),1}}{r\partial\theta}\right),$$

$$\varepsilon_{zr}^{(k),1}=\frac{1}{2}\left(\frac{\partial u_z^{(k),1}}{\partial r}+\frac{\partial u_r^{(k),1}}{\partial z}\right) \tag{10}$$

which coincide with the equations of the Three-Dimensional Linearised Theory of Elasticity (TDLTE) (Guz (1999)). It should be noted that the homogeneous parts of the equations obtained for the second and the subsequent approximations also coincide with the equations of the TDLTE.

Now we consider the contact conditions for each approximation, which are derived from equation (2). For this purpose, we substitute the expressions (6) and (7) into equation (2) and expand the components of each approximation of equation (6), i.e. expand the $\sigma_{rr}^{(k),q},...,u_r^{(k),q}$ in equation (6) in vicinity of (R,θ_k,t_3) into Taylor series. Then, grouping the terms with identical powers of the parameter ε and taking into account the foregoing assumptions, we derive the contact conditions for each approximation, e.g.,

1. for the zeroth approximation

$$[\sigma_{rr}]_{1,0}^{2k,0}=[\sigma_{r\theta}]_{1,0}^{2k,0}=[\sigma_{rz}]_{1,0}^{2k,0}=0,[u_r]_{1,0}^{2k,0}=[u_\theta]_{1,0}^{2k,0}=[u_z]_{1,0}^{2k,0}=0 \tag{11}$$

2. for the first approximation

$$[\sigma_{rr}]_{1,1}^{2k,1}+f_{1k}\left[\tfrac{\partial\sigma_{rr}}{\partial r}\right]_{1,0}^{2k,0}+\phi_{1k}\left[\tfrac{\partial\sigma_{rr}}{\partial z}\right]_{1,0}^{2k,0}+\gamma_{rk}[\sigma_{rr}]_{1,0}^{2k,0}+\gamma_{\theta k}[\sigma_{r\theta}]_{1,0}^{2k,0}+\gamma_{zk}[\sigma_{rz}]_{1,0}^{2k,0}=0$$

$$[u_r]_{1,1}^{2k,1}+f_{1k}\left[\frac{\partial u_r}{\partial r}\right]_{1,0}^{2k,0}+\phi_{1k}\left[\frac{\partial u_r}{\partial z}\right]_{1,0}^{2k,0}=0 \tag{12}$$

In equations (11) and (12) the following notation is used:
$[\mathrm{X}]_{1,q}^{2k,q}=\mathrm{X}^{(1),q}(R,\theta_k,t_3)-\mathrm{X}^{(2k),q}(R,\theta_k,t_3)$, q=0,1,

$$f_{1k}=\delta_k(t_3)\sin\theta_k,\phi_{1k}=-R\frac{d\delta_k(t_3)}{dt_3}\sin\theta_k, \tag{13}$$

$$\gamma_{rk} = \left(\frac{\delta_k(t_3)}{R} - \frac{d^2\delta_k(t_3)}{dt_3^2} R \right) \sin\theta_k, \gamma_{\theta k} = -\frac{\delta_k(t_3)}{R} \cos\theta_k, \gamma_{zk} = -\frac{d\delta_k(t_3)}{dt_3} \sin\theta_k.$$

In equation (12), only the contact relations for radial force $(\sigma_{rr} n_r + \sigma_{r\theta} n_\theta + \sigma_{rz} n_z)$ and radial displacement u_r are presented: the remaining ones are obtained by cyclic permutation of the indices r, θ and z in the components of the stress tensor (only the first index is replaced) and the displacement vector.

The zeroth approximation. Assume that the materials of each fiber are the same and Poisson coefficient of this material $\nu^{(21)} = \nu^{(22)}$ ($\nu^{(2k)}$ denotes Poisson coefficient of k.th fiber) is equal to Poisson coefficient of matrix material denoted by $\nu^{(1)}$.). This approximation has an exact analytical solution, which is given in Akbarov and Guz (2000), Guz (2003), Akbarov and Guz (1985), Akbarov and Mamedov (2009). According to these references, for $\nu^{(1)} = \nu^{(2k)}$, we have the following relations:

$$\varepsilon_{zz}^{(1),0} = \varepsilon_{zz}^{(21),0} = \varepsilon_{zz}^{(22),0} = \frac{p}{E^{(1)}}, \sigma_{zz}^{(1),0} = p, u_z^{(1),0} = u_z^{(21),0} = u_z^{(22),0} = \frac{p}{E^{(1)}} z,$$

$$u_r^{(1),0} = -\nu^{(1)} \varepsilon_{zz}^{(1),0} r, u_r^{(2k),0} = -\nu^{(2k)} \varepsilon_{zz}^{(2k),0} r, u_\theta^{(1),0} = u_\theta^{(2k),0} = 0,$$

$$\sigma_{rr}^{(1),0} = \sigma_{rr}^{(2k),0} = \sigma_{\theta\theta}^{(1),0} = \sigma_{\theta\theta}^{(2k),0} = 0, \sigma_{zz}^{(2k)} = p \frac{E^{(2k)}}{E^{(1)}},$$

$$\sigma_{\theta z}^{(1),0} = \sigma_{\theta z}^{(2k),0} = \sigma_{rz}^{(1),0} = \sigma_{rz}^{(2k),0} = \sigma_{r\theta}^{(1),0} = \sigma_{r\theta}^{(2k),0} = 0. \tag{14}$$

The first approximation. According to equations (14), equations (8) have the following form:

$$\frac{\partial \sigma_{rr}^{(k),1}}{\partial r} + \frac{1}{r} \frac{\partial \sigma_{r\theta}^{(k),1}}{\partial \theta} + \frac{\partial \sigma_{rz}^{(k),1}}{\partial z} + \frac{1}{r} \left(\sigma_{rr}^{(k),1} - \sigma_{\theta\theta}^{(k),1} \right) + \sigma_{zz}^{(\underline{k}),0} \frac{\partial^2 u_r^{(\underline{k}),1}}{\partial z^2} = 0,$$

$$\frac{\partial \sigma_{r\theta}^{(k),1}}{\partial r} + \frac{1}{r} \frac{\partial \sigma_{\theta\theta}^{(k),1}}{\partial \theta} + \frac{\partial \sigma_{\theta z}^{(k),1}}{\partial z} + \frac{2}{r} \sigma_{r\theta}^{(k),1} + \sigma_{zz}^{(\underline{k}),0} \frac{\partial^2 u_\theta^{(\underline{k}),1}}{\partial z^2} = 0,$$

$$\frac{\partial \sigma_{rz}^{(k),1}}{\partial r} + \frac{1}{r} \frac{\partial \sigma_{\theta z}^{(k),1}}{\partial \theta} + \frac{\partial \sigma_{zz}^{(k),1}}{\partial z} + \frac{1}{r} \sigma_{rz}^{(k),1} + \sigma_{zz}^{(\underline{k}),0} \frac{\partial^2 u_z^{(\underline{k}),1}}{\partial z^2} = 0, \tag{15}$$

The constitutive and geometrical relations (9) and (10) are remaining the same.

As for equations (14), the contact conditions for the first approximation assume the form

$$[\sigma_{rr}]_{1,1}^{2k,1} = 0, [\sigma_{r\theta}]_{1,1}^{2k,1} = 0, [\sigma_{rz}]_{1,1}^{2k,1} = \left(\sigma_{zz}^{(1),0} - \sigma_{zz}^{(2),0} \right) \frac{d\delta_k(t_3)}{dt_3} \cos\theta_k,$$

$$[u_r]_{1,1}^{2k,1} = 0, [u_\theta]_{1,1}^{2k,1} = 0, [u_z]_{1,1}^{2k,1} = 0. \tag{16}$$

For a solution to the problem (15), (9), (10), and (16), we employ the representations Guz (1999)

$$u_r = \frac{1}{r}\frac{\partial}{\partial\theta}\psi - \frac{\partial^2}{\partial r\partial z}\chi\,; u_\theta = -\frac{\partial}{\partial r}\psi - \frac{1}{r}\frac{\partial^2}{\partial r\partial z}\chi;$$

$$u_3 = (\lambda+\mu)^{-1}\left((\lambda+2\mu)\Delta_1 + \mu\frac{\partial^2}{\partial z^2}\right)\chi. \tag{17}$$

The functions of ψ and χ are determined from the equations

$$\left(\Delta_1 + \xi_1^2\frac{\partial^2}{\partial z^2}\right)\psi = 0;\ \left(\Delta_1 + \xi_2^2\frac{\partial^2}{\partial z^2}\right)\left(\Delta_1 + \xi_3^2\frac{\partial^2}{\partial z^2}\right)\chi = 0 \tag{18}$$

where

$$\xi_1 = \sqrt{\frac{\mu+\sigma_{zz}^0}{\mu}}, \xi_2 = \sqrt{\frac{\mu+\sigma_{zz}^0}{\mu}}, \xi_3 = \sqrt{\frac{\lambda+2\mu+\sigma_{zz}^0}{\lambda+2\mu}},$$

$$\Delta_1 = \frac{\partial^2}{\partial r^2} + \frac{1}{r}\frac{\partial}{\partial r} + \frac{1}{r^2}\frac{\partial^2}{\partial\theta^2}. \tag{19}$$

We apply the exponential Fourier transform with respect to z, i.e.

$$\overline{f}_{_F}(s) = \int_{-\infty}^{\infty} f(z)e^{-isz}dz \tag{20}$$

to the equations (9), (10), (15)- (18). After some mathematical manipulations we obtain

$$\overline{\psi}_F^{(2k)} = \sum_{n=-\infty}^{\infty}\overline{C}_n^{(2k)}(s)I_n\left(\frac{\xi_1^{(2k)}sr_k}{L}\right)\exp(in\theta_k)$$

$$\overline{\chi}_F^{(2k)} = i\sum_{n=-\infty}^{\infty}\left\{\left[\overline{A}_n^{(2k)}(s)I_n(\xi_2^{(2k)}s\frac{r_k}{L}) + \overline{B}_n^{(2k)}(s)I_n(\xi_3^{(2k)}s\frac{r_k}{L})\right]\right\}\exp(in\theta_k) \tag{21}$$

$$\overline{\psi}_F^{(1)} = \sum_{n=-\infty}^{\infty}\sum_{k=1}^{2}\overline{C}_n^{(1)k}(s)K_n(\xi_1^{(1)}s\frac{r_k}{L})\exp(in\theta_k)$$

$$\overline{\chi}_F^{(1),1} = i\left[\sum_{n=-\infty}^{\infty}\sum_{k=1}^{2}\left(\overline{A}_n^{(1)k}(s)K_n(\xi_2^{(1)}s\frac{r_k}{L}) + \overline{B}_n^{(1)k}(s)K_n(\xi_3^{(1)}s\frac{r_k}{L})\right)\exp(in\theta_k)\right] \tag{22}$$

where $I_n(x)$ are Bessel functions of a purely imaginary argument and $K_n(x)$are the Macdonald functions. Moreover the unknowns $\overline{A}_n^{(2k)},...,\overline{C}_n^{(2k)}$ are the complex constant and satisfy the relations:

$$\overline{A}_n^{(2k)} = \overline{\overline{A}_{-n}^{(2k)}},\ \overline{B}_n^{(2k)} = \overline{\overline{B}_{-n}^{(2k)}},\ \overline{C}_n^{(2k)} = \overline{\overline{C}_{-n}^{(2k)}}, Im\,\overline{A}_0^{(2k)} = Im\,\overline{B}_0^{(2k)} = Im\,\overline{C}_0^{(2k)} = 0,$$

$$\overline{A}_n^{(1)} = \overline{\overline{A}_{-n}^{(1)}},\ \overline{B}_n^{(1)} = \overline{\overline{B}_{-n}^{(1)}},\ \overline{C}_n^{(1)} = \overline{\overline{C}_{-n}^{(1)}}, Im\,\overline{A}_0^{(1)} = Im\,\overline{B}_0^{(1)} = Im\,\overline{C}_0^{(1)} = 0. \tag{23}$$

Now we attempt to satisfy the Fourier transforms of contact condition (16). For this purpose we must represent the expressions (22) and (23) in the k-th (k=1,2) cylindrical coordinate system to satisfy the contact conditions on the k-th fiber-matrix interface S_k. The expressions (21) are already presented in the k-th cylindrical system of coordinates. To make these operations for the expressions (22) we use the summation theorem (Watson (1962)) for the $K_n(x)$ function, which can be written for the case at hand as follows

$$r_m \exp i\theta_m = R_{mn} \exp i\phi_{mn} + r_n \exp i\theta_n,$$

$$K_\nu(cr_n)\exp i\nu\theta_n = \sum_{k=-\infty}^{\infty} (-1)^\nu I_k(cr_m)\, K_{\nu-k}(cR_{mn}) \exp[i(\nu-k)\phi_{mn}] \exp ik\theta_m,$$

$$mn = 12;21;\ m;n = 1,2;\ r_m < R_{mn};\ R_{12} = R_{21};\ \phi_{12} = 0;\ \phi_{21} = \pi \tag{24}$$

Now we specify equation (4) as

for cophase curving

$$x_{k1} = A\exp\left(-\left(\frac{x_{k3}}{L}\right)^2\right)\cos\left(m\frac{x_{k3}}{L}\right) = \varepsilon L\exp\left(-\left(\frac{x_{k3}}{L}\right)^2\right)\cos\left(m\frac{x_{k3}}{L}\right),$$

for antiphase curving

$$x_{k1} = (-1)^{k+1}A\exp\left(-\left(\tfrac{x_{k3}}{L}\right)^2\right)\cos\left(m\tfrac{x_{k3}}{L}\right) = (-1)^{k+1}\varepsilon L\exp\left(-\left(\tfrac{x_{k3}}{L}\right)^2\right)\cos\left(m\tfrac{x_{k3}}{L}\right),$$

$$x_{k2} = 0, \varepsilon = \frac{A}{L}, k = 1,2 \tag{25}$$

It is assumed that $L > A$, and the small parameter ε in (25) is introduced. Moreover, in (25) the following notation is used: A is the maximum value of the lift of the local curving and L is the introduced to be the geometrical parameter as shown in Fig. 1. In (25) the parameter m depicts the oscillatory character of the local mode of curvature.

Using (21)-(24) we obtain from Fourier transforms of (16) an infinite system of algebraic equations with respect to the unknown constants (23). Introducing the notation

$$\overline{C}_n^{(1)k} K_n(\xi_1^{(1)} s\frac{r_k}{L}) = y_{n1}^{(1)k} + iz_{n1}^{(1)k}, \overline{A}_n^{(1)k} K_n(\xi_2^{(1)} s\frac{r_k}{L}) = z_{n2}^{(1)k} + iy_{n2}^{(1)k},$$

$$\overline{B}_n^{(1)k} K_n(\xi_3^{(1)} s\frac{r_k}{L}) = z_{n3}^{(1)k} + iy_{n3}^{(1)k}, \overline{C}_n^{(2k)} I_n(\xi_1^{(2)} s\frac{r_k}{L}) = y_{n1}^{(2)k} + iz_{n1}^{(2)k},$$

$$\overline{A}_n^{(2k)} I_n(\xi_2^{(2)} s\frac{r_k}{L}) = z_{n2}^{(2)k} + iy_{n2}^{(2)k}, \overline{B}_n^{(2k)} I_n(\xi_3^{(2)} s\frac{r_k}{L}) = z_{n3}^{(2)k} + iy_{n3}^{(2)k},$$

$$Z_n^{(k)q} = \left\| \begin{array}{c} z_{n1}^{(k)q} \\ z_{n2}^{(k)q} \\ z_{n3}^{(k)q} \end{array} \right\|, Y_n^{(k)q} = \left\| \begin{array}{c} y_{n1}^{(k)q} \\ y_{n2}^{(k)q} \\ y_{n3}^{(k)q} \end{array} \right\|;$$

$$D_{nv}^{(1)q} = \left\| d_{rs}^{(1)q}(n,v) \right\|, D_n^{(2)q} = \left\| d_{rs}^{(2)q}(n) \right\|,$$

$$F_{nv}^{(1)q} = \left\| f_{rs}^{(1)q}(n,v) \right\|, F_n^{(2)q} = \left\| f_{rs}^{(2)q}(n) \right\|, i = \sqrt{-1}, q = 1,2; \text{k= } 1,2; r; s = 1,2,3, \tag{26}$$

we can unite this infinite set of equations in the following form:

$$Z_n^{(1)1} + \sum_{v=0}^{\infty} D_{nv}^{(1)2} Z_v^{(1)2} + D_n^{(2)1} Z_n^{(2)1} = 0, Z_n^{(1)2} + \sum_{v=0}^{\infty} D_{nv}^{(1)1} Z_v^{(1)1} + D_n^{(2)2} Z_n^{(2)2} = 0 \tag{27}$$

$$\begin{array}{l} Y_n^{(1)1} + \sum_{v=0}^{\infty} F_{nv}^{(1)2} Y_v^{(1)2} + F_n^{(2)1} Y_n^{(2)1} = \\ \qquad \delta_n^3 (\sigma_{zz}^{(1),0} - \sigma_{zz}^{(21),0}) s\frac{\sqrt{\pi}}{2} (\exp(-(\frac{s+m}{2})^2) - \exp(-(\frac{s-m}{2})^2)) \\ Y_n^{(1)2} + \sum_{v=0}^{\infty} F_{nv}^{(1)1} Y_v^{(1)1} + F_n^{(2)2} Y_n^{(2)2} = \\ \qquad \delta_n^3 (\sigma_{zz}^{(1),0} - \sigma_{zz}^{(22),0}) s\frac{\sqrt{\pi}}{2} (\exp(-(\frac{s+m}{2})^2) - \exp(-(\frac{s-m}{2})^2)) \end{array} \tag{28}$$

where $n = 1,2,...,\infty$, $\delta_3^3 = 1$ and $\delta_n^3 = 0$ for $n \neq 3$. Note that the component of the matrixes $D_{nv}^{(k)q}$, $F_{nv}^{(k)q}$, $D_n^{(2)q}$, $F_n^{(2)q}$ are obtained from the formulae Fourier transforms of (12)-(17) and (21)- (23). Due to cumbersome we omit here their detailed expressions.

It follows from (28) that $Z_n^{(k)q} = 0$, $k = 1,2$; $q = 1,2$. Moreover, it follows from the mechanical consideration and from the (23) the folllowing relations must be satisfied:

for co-phase curving case of the nanofibers

$$Y_n^{(1)1} = Y_n^{(1)2}, \tag{29}$$

for antiphase curving case of the nanofibers

$$Y_n^{(1)1} = -Y_n^{(1)2}, \tag{30}$$

Taking the relations, (29) and (30) into account from (28) we obtain for co-phase curving case
that $Y_n^{(k)1} = Y_n^{(k)2}$. Taking this into account, from (28) we obtain

$$\begin{array}{l} Y_n^{(1)1} + \sum_{v=0}^{\infty} F_{nv}^{(1)2} Y_v^{(1)1} + F_n^{(2)1} Y_n^{(2)1} = \\ \quad \delta_n^3 (\sigma_{zz}^{(1),0} - \sigma_{zz}^{(2),0}) s \frac{\sqrt{\pi}}{2} (\exp(-(\frac{s+m}{2})^2) - \exp(-(\frac{s-m}{2})^2)) \end{array} \tag{31}$$

and for antiphase curving case

$$\begin{array}{l} Y_n^{(1)1} - \sum_{v=0}^{\infty} F_{nv}^{(1)2} Y_v^{(1)1} + F_n^{(2)1} Y_n^{(2)1} = \\ \quad \delta_n^3 (\sigma_{zz}^{(1),0} - \sigma_{zz}^{(2),0}) s \frac{\sqrt{\pi}}{2} (\exp(-(\frac{s+m}{2})^2) - \exp(-(\frac{s-m}{2})^2)) \end{array} . \tag{32}$$

For numerical investigations the infinite system of algebraic equations (31) and (32) must be approximated by corresponding finite system. To validate of such a replacement, it must be shown that the determinant of the infinite system of equations is of normal type (Kantarovich and Krilov (1962)). Such is the case if the series

$$M = \sum_{n=0}^{\infty} \sum_{v=0}^{\infty} \left| F_{nv}^{(1)2} \right| \tag{33}$$

converges. For investigating this series, we use the following asymptotic estimates of the functions $I_n(x)$ and $K_n(x)$:

$$I_n(x) < c_1 \frac{1}{n!} \left(\frac{|x|}{2} \right)^n, c_1 = const.; K_n(x) \approx c_2 (n-1)! \left(\frac{2}{|x|} \right)^n, c_2 = const. \tag{34}$$

These relations hold for large n and fixed x. Let

$$\frac{R}{R_{12} - 2L} > \frac{R}{R_{12}}, \frac{R_{12}}{R} > 2 \tag{35}$$

which means that the fibres do not contact with each other. Then, taking into account equations (34) and (35) and analysing the expressions of $F_{nv}^{(1)2}$, we obtain the following estimate for series (33):

$$M < c_3 \sum_{n=0}^{\infty} n^{c_4} (\rho - 1)^{-n}; c_3, c_4 = const., \rho = \frac{R_{12}}{R} \tag{36}$$

As the series on the right hand side converges, so does series (33). Note that such a proof was also performed in Guz (1990), Guz, Rushchitsky and Guz (2007).

Consequently, for numerical investigations, the infinite system of algebraic equations (31) and (32) can be replaced with

$$\begin{array}{l} Y_n^{(1)1} + \sum_{v=0}^{N_v} F_{nv}^{(1)2} Y_v^{(1)1} + F_n^{(2)1} Y_n^{(2)1} = \\ \quad \delta_n^3 (\sigma_{zz}^{(1),0} - \sigma_{zz}^{(2),0}) s \frac{\sqrt{\pi}}{2} (\exp(-(\frac{s+m}{2})^2) - \exp(-(\frac{s-m}{2})^2)) \end{array} \tag{37}$$

for the cophase curving case and with

$$\begin{array}{l} Y_n^{(1)1} - \sum_{v=0}^{N_v} F_{nv}^{(1)2} Y_v^{(1)1} + F_n^{(2)1} Y_n^{(2)1} = \\ \quad \delta_n^3 (\sigma_{zz}^{(1),0} - \sigma_{zz}^{(2),0}) s \frac{\sqrt{\pi}}{2} (\exp(-(\frac{s+m}{2})^2) - \exp(-(\frac{s-m}{2})^2)) \end{array} . \tag{38}$$

for the antiphase curving case, where $n = 1, 2, ..., N_v$ in equations (37) and (38). The values of N_v in these equations are determined from the convergence requirement of numerical results.

Using the Fourier transforms to equations. (9), (10) we obtain the expressions for $\bar{\sigma}_{rrF}^{(1),1}, ..., \bar{\sigma}_{zzF}^{(2),1}$. The inverse transform for the stresses, for example, for the stress $\sigma_{rr}^{(1),1}$ is determined by

$$\sigma_{rr}^{(1),1} = \frac{1}{2\pi} \int_{-\infty}^{+\infty} \bar{\sigma}_{rrF}^{(1),1} e^{isz} ds \tag{39}$$

Equation (25) shows that the selected function $\delta_k(t_3)$ is even one and therefore the expression (37) can be replaced with

$$\sigma_{rr}^{(1),1} = \frac{1}{\pi} \int_{0}^{+\infty} \bar{\sigma}_{rrF}^{(1),1} \cos z ds \tag{40}$$

By similar manner we obtain the expressions to calculate the other sought values.

Thus, by the above-described method we determine completely the values of the first approximation. Note that the values of the second and subsequent approximations in equation (6) can also be determined by this method. According to the investigations analyzed in Akbarov and Guz (2000) the main effect of the fibers curving on stress distribution arises within the framework of the first approximation. The second and subsequent approximations give only some insignificant quantitative corrections to these results. However, to determine of the values of these approximations requires some very complicated and cumbersome mathematical procedures. Taking the above stated into account the investigations in the present paper are made only within the framework of the zeroth and first approximations.

4 Numerical Results and Discussions

First, we consider some remarks on the calculation of the improved integral (40). Note that under the calculation procedure these improved integrals are replaced by

the corresponding definite ones, i.e. we use the relation $\int_0^{+\infty}(.)ds \cong \int_0^{S_*}(.)ds = \sum_{i=0}^{N}\int_{S_i}^{S_{i+1}}(.)ds$, $S_0 = 0$, $S_N = S_*$. The values of N and S_* are determined from the convergence criterion of the improved integrals. Further, for the calculation of the integrals $\int_{S_i}^{S_{i+1}}(.)ds$ the Gauss integration algorithm is employed. All these procedures are made automatically in PC by using programmes written in FTN77.

As follows from the present investigations and those carried out in the monograph Akbarov and Guz (2000) that in the sinphase (antiphase) curving case the shear (normal) stress $\sigma_{n\tau}$ (σ_{nn}) has dominating values. Taking above-stated into account we consider the influence of the problem parameter to the values of $\sigma_{n\tau}$ in the cophase curving case, but in the antiphase curving case we investigate this influence for the normal stress σ_{nn}. Moreover, the aforementioned investigations show that the stresses σ_{nn} and $\sigma_{n\tau}$ have a maximum at the point $\theta = 0$ determined by equation (5). In view of corresponding symmetry we consider the distribution of these stresses only for $x_3 \geq 0$ and $0 \leq \theta \leq \pi$ (Fig. 1). Note that the stresses $\sigma_{n\tau}$ and σ_{nn} act along the tangent vectors τ and the normal vector n to the surface of the fiber, respectively. If $\varepsilon = 0$ (i.e. if the curving is absent), the stresses σ_{nn} and $\sigma_{n\tau}$ coincide with σ_{rr} and σ_{rz}, respectively.

We introduce the parameters $\kappa = R/L$, $\rho = R_{12}/R$ where R is a radius of the cross-section of the fibers, R_{12} is a distance between two neighboring fibers (Fig. 1), and unless otherwise specified, assume that $\varepsilon = 0.07$, $m = 1$, $x_3/L = 0.7$ in calculating the values of $\sigma_{n\tau}/|p|$, $x_3/L = 0$ in calculating the values of $\sigma_{nn}/|p|$, $\nu^{(1)} = \nu^{(2)} = 0.3$, $E^{(2)}/E^{(1)} = 500$ where $E^{(2)}$and $E^{(1)}$ ($\nu^{(2)}$and $\nu^{(1)}$) are Young's moduli (Poisson ratio) of nanofibers and matrix materials, respectively. To illustrate the influence of the geometrical nonlinearity on the distribution of the considered stresses we will use the parameter $\alpha = p/E^{(1)}$.

Thus, consider the graphs given in Figs. 2 and 3 which show the dependencies between the $\sigma_{n\tau}/|p|$ and the parameter κ for $\rho = 2.1$ and 2.5, respectively, for various suitible values of the parameter α. The graphs of the dependencies between $\sigma_{nn}/|p|$ and κ with the same sequencies of the problem parameters are given in Figs. 4 and 5. In these figures the graphs denoted by (a) and (b) correspond to the tension and compression of the consireded body, respectively. Note that under the consideration of compression we assume that $|\alpha| < |\alpha_{cr.}|$, where $\alpha_{cr.}$ is the critical values of the parameter α obtained for the stability loss problem of the two neighboring locally curved of fibers in an infinite matrix. The numerical results given in the foregoing figures show that the dependencies among $\sigma_{n\tau}/|p|$, $\sigma_{nn}/|p|$ and κ have non-monotonic character, i.e. there is such value of the parameter κ (denote it by κ^*) under which the absolute values of the considered stresses have its absolute maximum.

According to the numerical results, the values of κ^* decrease with increasing ρ (i.e.

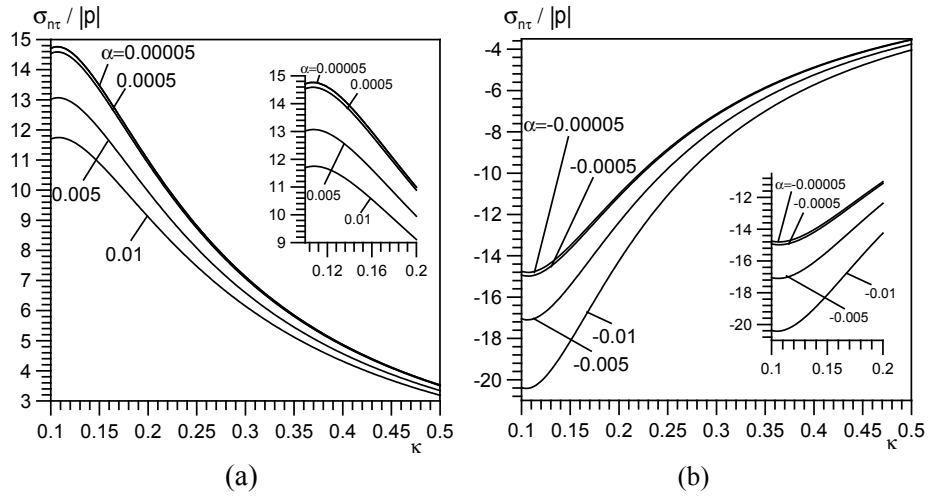

Figure 2: The graphs of the dependencies between $\sigma_{n\tau}/|p|$ and parameter κ for various values of α under $\rho = 2.1$ a) tension b) compression

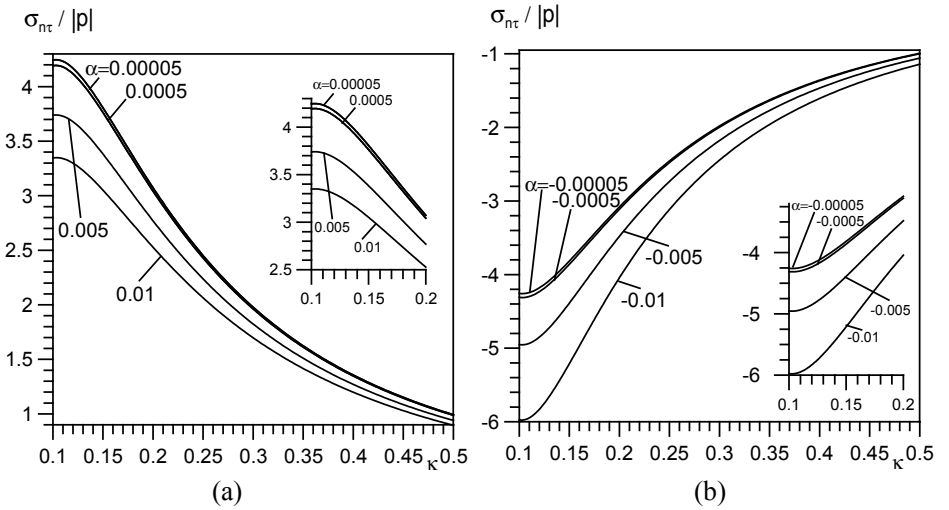

Figure 3: The graphs of the dependencies between $\sigma_{n\tau}/|p|$ and parameter κ for various values of α under $\rho = 2.5$ a) tension b) compression

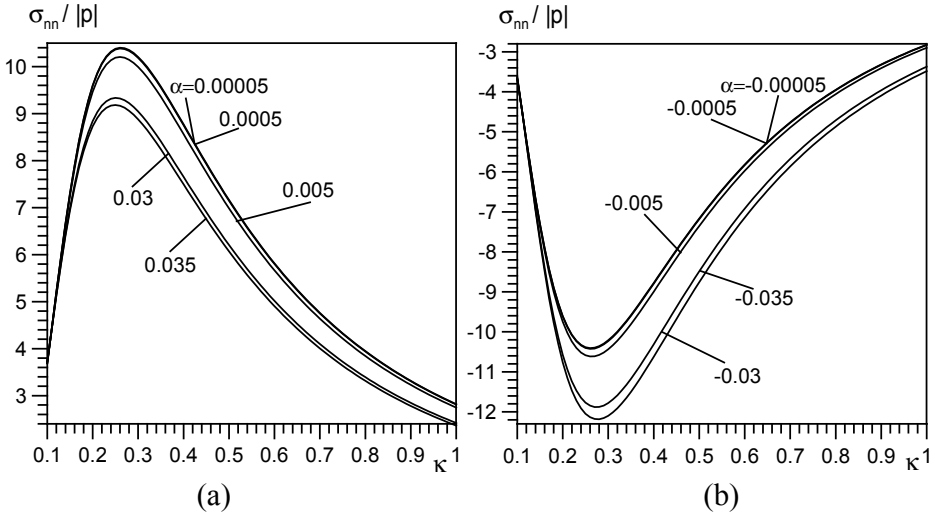

Figure 4: The graphs of the dependencies between $\sigma_{nn}/|p|$ and parameter κ for various values of α under $\rho = 2.1$ a) tension b) compression

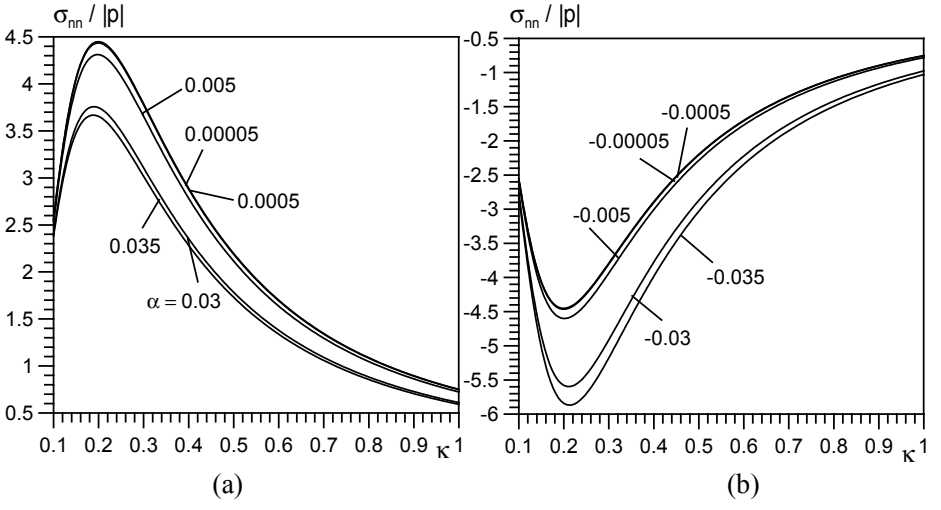

Figure 5: The graphs of the dependencies between $\sigma_{nn}/|p|$ and parameter κ for various values of α under $\rho = 2.1$ a) tension b) compression

with increasing the distance between the two neighboring fibers). Absolute maximum values of $\sigma_{n\tau}/|p|$ in the cophase curving case and absolute maximum values of $\sigma_{nn}/|p|$ in the antiphase curving case increase with decreasing ρ. In this case, as a result of the geometrical non-linearity the absolute values of $\sigma_{n\tau}/|p|$ and $\sigma_{nn}/|p|$ decrease (increase) under tension (compression) with the parameter $|\alpha|$. It follows clearly from the foregoing numerical results that the maximum effect of the influence of the geometrical non-linearity arise for the cases where $\kappa = \kappa^*$. Moreover, this effect increases with increasing ρ. Note that the numerical results obtained under compression and tension in the case where $\alpha = \pm 0.00005$ coincide with each other. This situation also agree well with the mechanical consideration and confirm the trustness of the algorithm and programms used in the present numerical investigations.

Consider the influence of the parameter m (Eq. (25)) which characterises the oscillation of the local curving form of the fibers on the distrubitions of the stress $\sigma_{n\tau}/|p|$ and $\sigma_{nn}/|p|$ with respect to x_3/L. This influence is shown by the graphs given in Figs. 6 and 7 under $\kappa = 0.25$, $\rho = 2.1$ (a) $\alpha = 0.01$, (b) $\alpha = -0.01$. It follows from these graphs that the absolute maximum value of the considered normal and shear stresses increase with m. These results agree in the qualitative sense with the corresponding ones analyzed in monograph Akbarov and Guz (2000).

Consider the graphs given in Figs. 8 and 9 which illustrate the influences of the interaction between the fibers to considered stress distribution. These figures show us the dependencies between $\sigma_{n\tau}/|p|$, $\sigma_{nn}/|p|$ and ρ under $m = 1$, $x_3/L = 0.7$ (for$\sigma_{n\tau}/|p|$), $x_3/L = 0$ (for $\sigma_{nn}/|p|$), $\kappa = 0.25$. It follows from the foregoing numerical results that absolute value of $\sigma_{n\tau}$ and σ_{nn} increase with decreasing ρ. In this case, as a result of the geometrical non-linearity the absolute values of σ_{nn} and $\sigma_{n\tau}$ decrease (increase) under tension (compression) with increasing the parameter $|\alpha|$. Note that the numerical results obtained under compression and tension in the case where $\alpha = \pm 0.00005$ coincide with each other and with increasing ρ, these results approach to the corresponding ones obtained in Akbarov, Kosker and Simsek (2005) for a single locally curved fiber. According to the values stresses attained for microfibers+polymer matrix system and for nanofibers+polymer matrix system, to compare which results approach to the values of stresses obtained for a single locally curved fiber faster, we investigate the effect of parameter $E^{(2)}/E^{(1)}$on considered stresses distributions.

For this purpose, figs. 10 and 11 are given. These figures show the dependencies between $\sigma_{n\tau}/|p|$, $\sigma_{nn}/|p|$ and parameter $E^{(2)}/E^{(1)}$under $m = 1$, $x_3/L = 0.7$ (for$\sigma_{n\tau}/|p|$), $x_3/L = 0$ (for $\sigma_{nn}/|p|$), $\kappa = 0.25$., a) $\alpha = 0.01$ b) $\alpha = -0.01$. It follows from these figures that the values of self-balanced normal and shear stresses obtained for microfibers+polymer matrix system approach to the corresponding

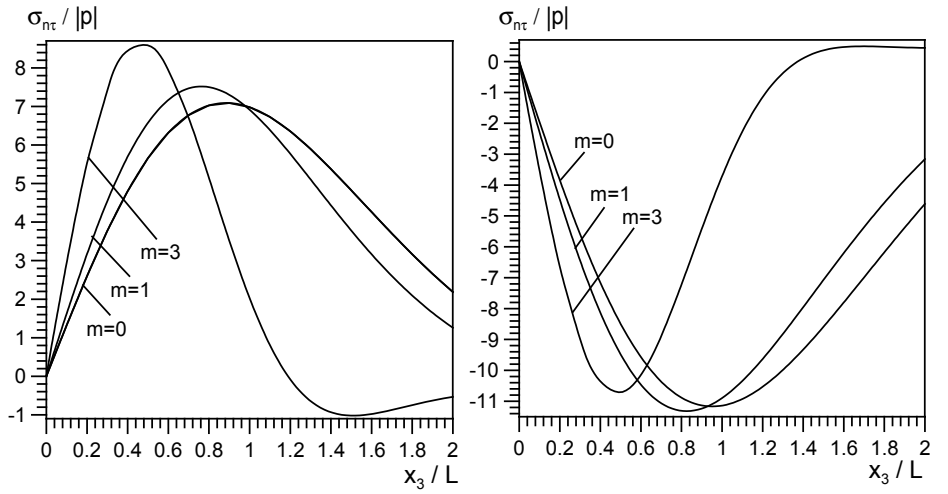

Figure 6: The graphs of the dependencies between $\sigma_{n\tau}/|p|$ and parameter x_3/L for various values of m under $\rho = 2.1$, $\kappa = 0.25$, a) $\alpha = 0.01$, b) $\alpha = -0.01$

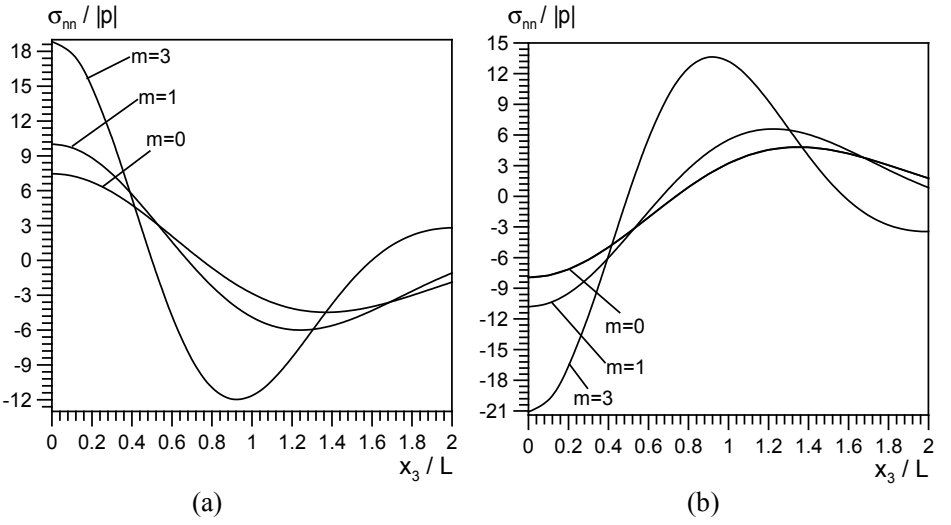

Figure 7: The graphs of the dependencies between $\sigma_{nn}/|p|$ and parameter x_3/L for various values of m under $\rho = 2.1$, $\kappa = 0.25$, a) $\alpha = 0.01$, b) $\alpha = -0.01$

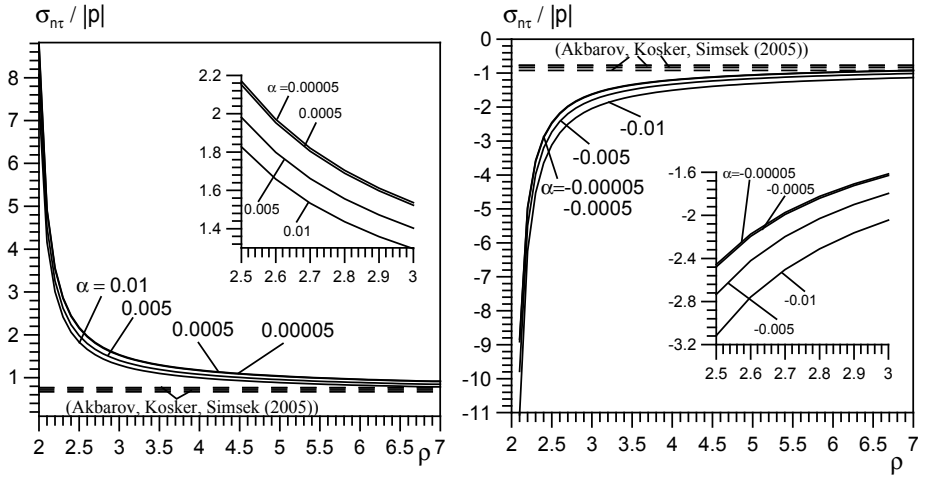

Figure 8: The graphs of the dependencies between $\sigma_{n\tau}/|p|$ and parameter ρ for various values of α under $\kappa = 0.25$, a) tension b) compression.

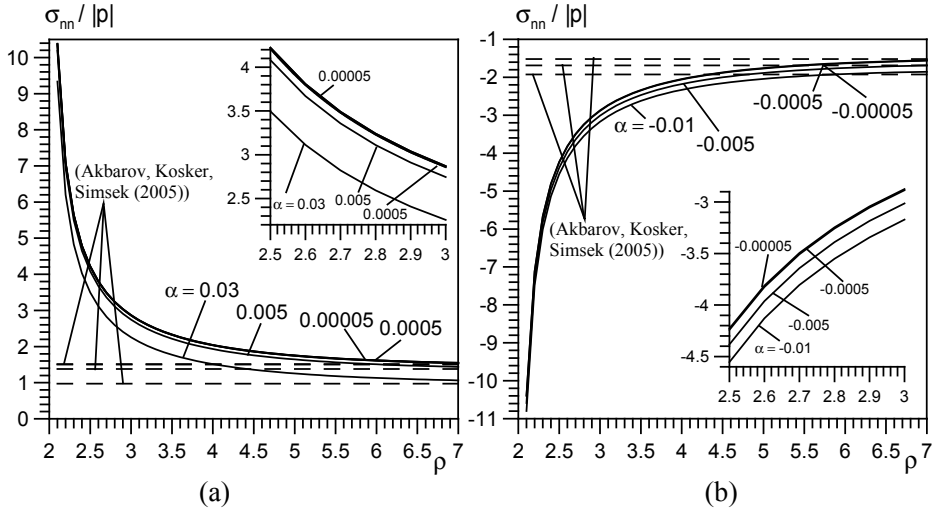

Figure 9: The graphs of the dependencies between $\sigma_{nn}/|p|$ and parameter ρ for various values of α under $\kappa = 0.25$ a) tension b) compression.

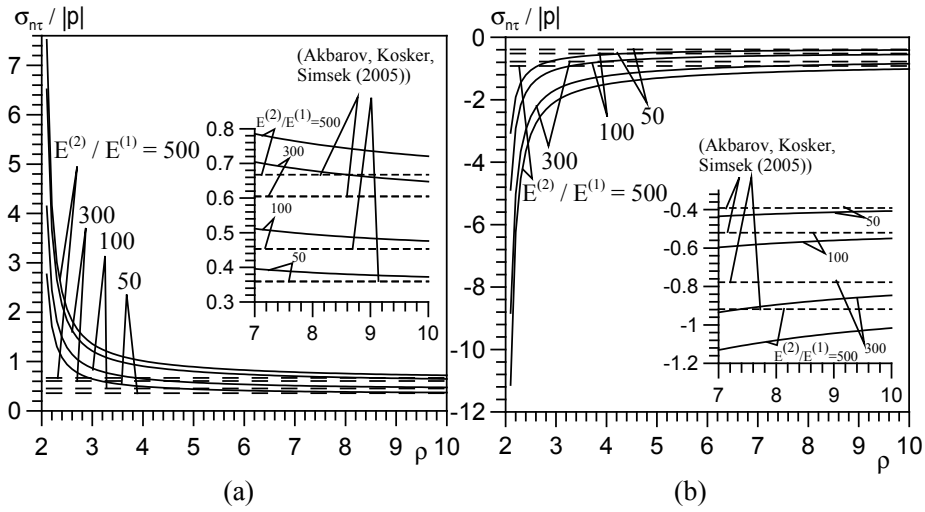

Figure 10: The graphs of the dependencies between $\sigma_{n\tau}/|p|$ and parameter ρ for various values of $E^{(2)}/E^{(1)}$ under $\kappa = 0.25$, a) $\alpha = 0.01$ b) $\alpha = -0.01$.

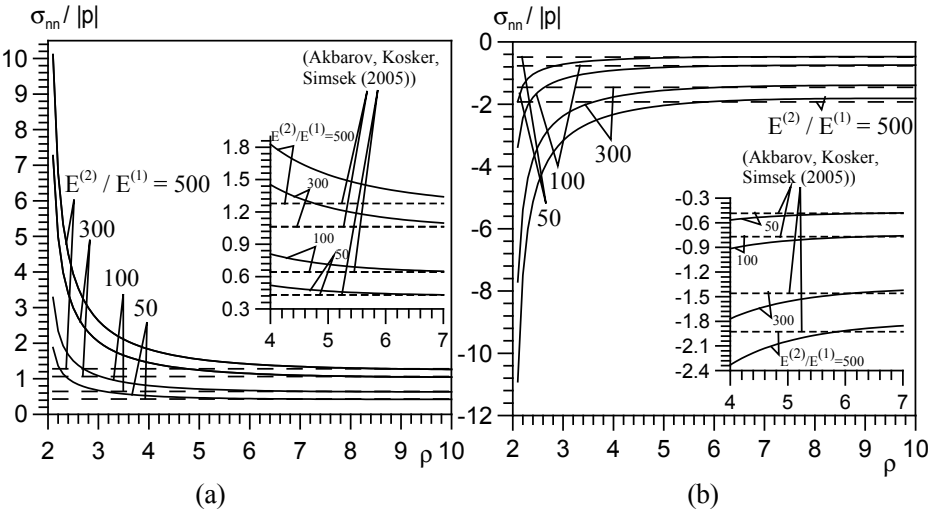

Figure 11: The graphs of the dependencies between $\sigma_{nn}/|p|$ and parameter ρ for various values of $E^{(2)}/E^{(1)}$ under $\kappa = 0.25$, a) $\alpha = 0.01$ b) $\alpha = -0.01$.

ones attained for a single locally curved fiber, faster than the values of stresses obtained for nanofibers+polymer matrix system.

Consider Tables 1 and 2 which show the values of $\sigma_{n\tau}/|p|$ (for the cophase curving case) and $\sigma_{nn}/|p|$ (for the antiphase curving case) respectively obtained for various α, ρ and $E^{(2)}/E^{(1)}$ under $\kappa = 0.25$, $m = 1$,$x_3/L = 0.7$ (for$\sigma_{n\tau}/|p|$), $x_3/L = 0$ (for $\sigma_{nn}/|p|$). It follows from these tables that the influence of the geometrical non-linearity to the values of the considered stresses increase and the interaction between the fibers becomes more considerable with $E^{(2)}/E^{(1)}$.

Moreover, table 3 illustrates the convergence of the numerical results in the first approximation with respect to the number of the selected equations (N_ν in equations (37) and (38)). The numerical results given in this table are obtained under $E^{(2)}/E^{(1)} = 500$, $\rho = 2.1$, $\alpha = 5.10^{-5}$, $\kappa = 0.25$, $m = 1$,$x_3/L = 0.7$ (for$\sigma_{n\tau}/|p|$), $x_3/L = 0$ (for $\sigma_{nn}/|p|$). It follows from these table that the convergence of the used solution method is adequate.

5 Conclusions

In the present paper, the stress distribution in an infinite elastic body containing two neighboring nanofibers is studied. The nanofiber is modeled within the scope of the continuum approach with high modulus of elasticity. It is assumed that the midlines of the fibers are in the same plane. With respect to the location of the fibers according to each other the co-phase and anti-phase curving cases are considered. At infinity uniformly distributed normal forces act in the direction of the nanofibers' location. The investigations are carried out in the framework of the piecewise homogeneous body model with the use of the three-dimensional geometrically non-linear exact equations of the theory of elasticity.

The numerical results, related to the self-balanced shear (for the cophase curving case) and normal (for the antiphase curving case) stresses which act on the interface and arises as a result of the fiber curving, are given. In this case, the influence of the geometrical non-linearity to these stresses is analyzed. From the analyses of these results are derived the following conclusions:

1. As a result of the geometrical non-linearity, the absolute values of the considered stresses increase in compression but decrease in tension.

2. The maximum effect of the geometrical non-linearity to the stresses arises under certain values of κ.

3. The effect of the geometrical non-linearity to the considered stresses increases with $E^{(2)}/E^{(1)}$ (where $E^{(2)}$ ($E^{(1)}$) Young's moduli of the fibers (matrix) material).

Table 1: The values of $\sigma_{n\tau}/|p|$ obtained in the cophase curving case for various values of $E^{(2)}/E^{(1)}$, α and ρ under $\kappa = 0.25$, $m = 1$, $x_3/L = 0.7$.

ρ	$\alpha = \frac{p}{E^{(1)}}$	$E^{(2)}/E^{(1)}$		
		300	400	500
2.1	0.00005	7.14461	8.20092	8.45786
	0.00050	7.09760	8.13822	8.38757
	0.00500	6.66738	7.57202	7.75901
	0.01000	6.47241	7.04842	7.46980
	0.01500	6.10766	6.60863	6.96901
	-0.00005	-7.15516	-8.21502	-8.47369
	-0.00050	-7.20314	-8.27925	-8.54587
	-0.00500	-7.73263	-9.00035	-9.36711
	-0.01000	-8.77625	-10.0219	-11.06459
	-0.01500	-9.74652	-11.4035	-12.90081
2.5	0.00005	2.03918	2.30525	2.34981
	0.00050	2.02503	2.28676	2.32943
	0.00500	1.89607	2.12059	2.14807
	0.01000	1.83678	1.96813	2.06352
	0.01500	1.72885	1.84093	1.92091
	-0.00005	-2.04236	-2.30941	-2.35440
	-0.00050	-2.05682	-2.32838	-2.37535
	-0.00500	-2.21733	-2.54262	-2.61532
	-0.01000	-2.53516	-2.85061	-3.11534
	-0.01500	-2.83912	-3.27657	-3.67646
3	0.00005	1.34896	1.51895	1.54638
	0.00050	1.33966	1.50686	1.53309
	0.00500	1.25497	1.39816	1.41470
	0.01000	1.21532	1.29835	1.35868
	0.01500	1.14438	1.21503	1.26547
	-0.00005	-1.35104	-1.52167	-1.54938
	-0.00050	-1.36054	-1.53406	-1.56304
	-0.00500	-1.46588	-1.67403	-1.71945
	-0.01000	-1.67352	-1.87494	-2.04392
	-0.01500	-1.87241	-2.15213	-2.40744

4. The absolute values of the self-balanced normal and shear stresses arising as a result of the local curving of the neighboring two nanofibers are significantly greater than the corresponding values obtained for the microfibers (Akbarov, Kosker and Simsek (2005)).

5. The values of κ ($\kappa = R/L$, R is a radius of the cross-section of the fibers, L

Table 2: The values of $\sigma_{nn}/|p|$ obtained in the cophase curving case for various values of $E^{(2)}/E^{(1)}$, α and ρ under $\kappa = 0.25$, $m = 1$, $x_3/L = 0$.

ρ	$\alpha = \frac{p}{E^{(1)}}$	$E^{(2)}/E^{(1)}$		
		300	400	500
2.1	0.00005	7.39540	8.97866	10.3803
	0.00050	7.38575	8.96494	10.3625
	0.00500	7.29089	8.83050	10.1884
	0.01000	7.18894	8.68675	10.0030
	0.01500	7.09041	8.54854	9.82557
	-0.00005	-7.39755	-8.98172	-10.3843
	-0.00050	-7.40724	-8.99550	-10.4025
	-0.00500	-7.50593	-9.13625	-10.5854
	-0.01000	-7.61950	-9.29916	-10.7984
	-0.01500	-7.73747	-9.46944	-11.0223
2.5	0.00005	3.16556	3.73519	4.22442
	0.00050	3.15743	3.72432	4.21094
	0.00500	3.07863	3.61943	4.08119
	0.01000	2.99615	3.51042	3.94710
	0.01500	2.91854	3.40853	3.82247
	-0.00005	-3.16738	-3.73761	-4.22744
	-0.00050	-3.17557	-3.74857	-4.24104
	-0.00500	-3.26027	-3.86229	-4.38274
	-0.01000	-3.36070	-3.99823	-4.55330
	-0.01500	-3.46856	-4.14559	-4.73692
3	0.00005	2.19619	2.5610	2.87103
	0.00050	2.18872	2.5512	2.85904
	0.00500	2.11700	2.4576	2.74489
	0.01000	2.04319	2.3621	2.62922
	0.01500	1.97486	2.2744	2.52372
	-0.00005	-2.19785	-2.5632	-2.87371
	-0.00050	-2.20359	-2.5731	-2.88584
	-0.00500	-2.28411	-2.6769	-3.01367
	-0.01000	-2.37391	-2.8039	-3.17130
	-0.01500	-2.48390	-2.9450	-3.34843

Table 3: The values of $\sigma_{n\tau}/|p|$ ($\sigma_{nn}/|p|$) obtained in the cophase (antiphase) curving case for various values of N_v in equations (37) and (38) in the case where $E^{(2)}/E^{(1)} = 500$, $\rho = 2.1$, $\alpha = 5.10^{-5}$, $\kappa = 0.25$, $m = 1$, $x_3/L = 0.7$

stresses	Number of equations (N_v)						
	28	40	52	64	76	88	94
$\sigma_{n\tau}/\|p\|$	6.0412	7.2438	7.8445	8.1828	8.3470	8.4302	8.4579
$\sigma_{nn}/\|p\|$	6.6527	8.3327	9.3171	9.8688	10.1693	10.3306	10.3804

is a geometrical parameter as shown in Fig.1), under which the considered stresses have its absolute maximum values obtained for the system consisting of nanofiber and polymer matrix, are significantly less than corresponding ones obtained for the microfibers+polymer matrix system.

6. It follows from the numerical results that the stresses caused by the local curving of the nanofibers can be debonded from matrix material.

7. The obtained numerical results can be used for estimation of the adhesion strength of the nanofiber+polymer composite materials.

8. The values of self-balanced normal and shear stresses obtained for microfibers+polymer matrix system approach to the corresponding ones attained for a single locally curved fiber, faster than the values of stresses obtained for nanofibers+polymer matrix system.

Obtained numerical results agree well with the well-known mechanical consideration and in the particular cases coincide with the corresponding known results.

References

Akbarov, StateS.D. (2007): Three-dimensional stability loss problems of the viscoelastic composite materials and structural members. *Int. Appl. Mech*., Vol.43, No 10, 3-27.

Akbarov, S. D.; Guz, A. N. (1985a): Method of solving problems in the mechanics of fiber composites with curved structures. *Int. Appl. Mech.* vol.21, pp.777-785.

Akbarov, S. D.; Guz, A. N. (1985b): Stress state of fiber composite with curved structures with a low fiber concentration. *Int. Appl. Mech.* vol 21, pp. 560-565.

Akbarov, S. D.; Guz, A. N. (2000): *Mechanics of curved composites.* Kluwer Academic Pubishers, Dortrecht/Boston/London. pp. 464.

Akbarov, S. D.; Guz, A. N. (2002): Mechanics of curved composites (piecewise homogenous body model). *Int. Appl. Mech.*, 38, No:12, 1415-1439.

Akbarov, S. D.; Guz, A. N. (2004): Mechanics of curved composites and some related problems for structural members. *Mechanics of Advanced Materials and Structures*. Vol. 11, pp. 445-515.

Akbarov, S. D.; Kosker, R. (2003a): Stress distribution caused by antiphase periodical curving of two neighboring fibers in a composite materials. *Eur. J. Mech. A/ Solids.* Vol.22, pp. 243-256.

Akbarov, S. D.; Kosker, R. (2003b): On the stress analyses in the infinite elastic body with two neighbouring curved fibers. *Composites, Part B: Engineering*. vol. 34 (2), pp. 143-150.

Akbarov, S. D.; Kosker, R. (2004): Internal stability loss of two neighbouring fibers in a viscoelastic matrix. *Int. J. Eng. Scien.* Vol.42 (17/18), pp.1847-1873.

Akbarov, S. D.; Kosker, R.; Simsek, K. (2005): Stress distribution in an infinite elastic body with a locally curved fiber in a geometrically nonlinear statement. *Mechanics of Composite Materials*, 41 (4): 291-302.

Akbarov, S. D.; Kosker, R.; Ucan Y. (2004): Stress distribution in an elastic body with a periodically curved row of fibers. *Mech. Compos. Mater.* Vol.40(3), pp. 191-202.

Akbarov, S. D.; Kosker, R.; Ucan, Y. (2006): Stress distribution in a composite material with the row of anti-phase periodically curved fibers. *Int. Appl. Mech.*, vol.42(4), pp. 486-493.

Akbarov, S. D.; Kosker, R.; Ucan Y. (2010): The Effect of the Geometrical Nonlinearity on the Stres Distribution in the Infinite Elastic Body with a Periodically Curved Row of Fibers. *CMC: Computers, Materials & Continua*. Vol. 17, No. 2, pp. 77-102.

Akbarov, S. D.; Mamedov, A. R. (2009): On the solution method for problems related to the micro-mechanics of a periodically curved fiber near a convex cylindrical surface. *CMES: Computer Modeling in Engineering and Sciences*, vol. 42(3), pp. 257-296.

Chou, T.W.; McCullough, R.L.; Pipes, R.B. (1986); Composites. *Journal Scientific American*. No 10, pp. 193-203.

Cinar, N. T.; Kosker, R.; Akbarov, S. D.; Akat, E. (2010): Stress distribution caused by two neighboring out-of-plane locally cophasally curved fibers in a composite material. *Mechanics of Composite Materials*, Vol. 46, No. 5, pp.555-572.

Corten, H. T. (1967): *Fracture of reinforcing plastics*. In L. J. Broutman and R:H: Krock (eds.). Modern Composite Materials, pp.27-100, Addison-Wesley, Reading, MA.

Djafarova, E.K. (1992): On the solution method of the stress-strain state problems in the fibrous composites with locally curving structures, *Tr. Nauch. Konf. Molod. Uchyon. In-ta Mekhan. AN Ukr*., Kiew, Part I. pp.39-44 (in Russian).

Djafarova, E.K. (1994): *Distribution of self-equilibrated stresses in fibrous composite materials with local curving in the structures.* Dep. In VINITI, N 2166-B94, 34p (in Russian).

Djafarova, E.K. (1995): *Stress state in composite materials with local curving fibers.* Dissertation for the degree of Candidate of Physico-Mathematical Sciences. Inst. Methem. And Mekhan. AN Azerb. Republ. Baku, 110p (in Russian).

Feng, Z. -N.; Allen, H. G.; Moy, S. S. (1998): Micromechanical analyses of a woven composite. *In Proc. ECCM -8*, Wood Head Publishing Limited, Naples, Italy, vol. 4, pp. 619-625.

Ganesh, V. K.; Naik, N. K. (1996): Failure behavior of plane weave fabric laminates under on- axis uniaxial tensile loading, III –effect of fabric geometry. *J. Compos. Mater.* vol.30, pp. 1823-1856.

Guz, A. N. (1999): *Fundamentals of the Three-Dimensional Theory of Stability of Deformable Bodies*. Springer-Verlag, Berlin Heideberg, pp. 556.

Guz, A. N. (1990): *Failure mechanics of composite materials in compression*. Kiew:Naukova Dumca (in Russian).

Guz, A. N. (2003): On one two-level model in the mesomechanics of compression fracture of Cracked Composites. *Int. Appl. Mech.*, 39, No:3, 274-285.

Guz, A. N. (2006): The Three- Dimensional Theory of Stability of a Carbon Nanotube. *Int. Appl. Mech.,*, 42(1), pp.19-31.

Guz, A.N.; Dekret, V.A. (2008): On two models in the three-dimensional theory of stability of composites. *Int. Appl. Mech.*, 44(8), pp.839-854.

Guz, A. N.; Lapusta, Yu. N. (1986): Stability of a fiber near a free surface. *Int. Appl. Mech.* Vol. 22 (8), pp. 711-719.

Guz, A.N; Rushchitsky, J.J.; Guz, I.N. (2007): Establishing fundamentals of the Mechanics of Nanocomposites. *Int. Appl. Mech.,* 43(3), pp.247-269.

Kantarovich, L. V., Krilov, V. I. (1962): *Approximate methods in advanced calculus.* Moscow: Fizmatgiz, (in Russian), pp. 708.

Kosker, R.; Akbarov, S. D. (2003): Influence of the interaction between periodically curved fibers on the stress distribution in a composite material. *Mech.*

Compos. Mater. Vol. 39(2), pp.165-176.

Kosker, R.; Cinar, N.T. (2009): Stress Distribution in an Infinite Elastic body Containing Two Neighboring Locally Curved Fibers, *Mech. Compos. Mater.*, Vol 45(3), pp.315-330.

Maligino, A.R.; Warrior, N.A.; Long, A.C. (2009): Effect on inter-fibre spacing on damage evolution in unidirectional (UD) fibre-reinforced composites. *Eur. J. Mech. A.Solids*., 28, pp.768-776.

Qian, D.; Dickey, E.C.; Andrews, R.; Rantell, T. (2000): Load transfer and deformation mechanisms of carbon nanotube-plytyrene composites. *Appl. Phys. Lett,*. Vol 76(20),pp.2868-2870.

Tarnopolsky, Yu. M.; Jigun, placeI. G.; Polyakov, V. A. (1987): *Spatially-reinforcedcomposite materials: Handbook*. Mashinostroyenia, Moscow. (in Russian).

Tomashevskii, V.T.; Yakovlev, V.S. (2004): Models in the Engineering Mechanics of Polymer-Matrix Systems. *Int. Appl. Mech*.,40, No. 6, pp.601-621.

Watson, G. M. (1962): *A Treatise on the Theory of Bessel functions.* Second Edition, Cambridge at the University Press, pp. 804.

Zhuk, Yu. A.; Guz, placeI. A.(2007): Features of plane wave propagation along the layers of a pre-strained nanocomposites. *Int. Appl. Mech.*, 43(4), pp.361-379.